COMMUNICATIONS IN NUMERICAL METHODS IN ENGINEERING
Commun. Numer. Meth. Engng 2004; **20**:353–361 (DOI: 10.1002/cnm.678)

Numerical error patterns for a scheme with Hermite interpolation for $1 + 1$ linear wave equations

Zuojin Zhu*,†, Xiangqi Wang and Zhenbi Su

Department of Thermal Science and Energy Engineering, University of Science and Technology of China, Anhui, Hefei, 230026, People's Republic of China

SUMMARY

Numerical error patterns were presented when the fourth-order scheme based on Hermite interpolation was used to solve the $1 + 1$ linear wave equation. Since most non-linear equations for real systems can be converted into linear forms by using proper transformations, this study certainly pertains its practical significance. The analytical solution was obtained under inhomogeneous initial and boundary conditions. It was found that not only the Hurst index of an error train at a given position but also its spatial distribution is dependent on the ratio of temporal to spatial intervals. The solution process with the fourth-order scheme based on Hermite interpolation diverges as the ratio is greater than unity. The results show that regular error pattern and smaller *maxima* of absolute values of numerical errors can be obtained when the ratio is set as unity; while chaotic phenomena for the numerical error propagation process can appear when the ratio is less than unity. It was found that it is better to choose the ratio as unity for the numerical solution of $1 + 1$ linear wave equation with the scheme; while other selections for the ratio in the scheme can bring about chaotic patterns for the numerical errors. Copyright © 2004 John Wiley & Sons, Ltd.

KEY WORDS: scheme based on Hermite interpolation; wave equation; numerical error pattern

1. INTRODUCTION

Error spreading behaviour is an important feature currently absorbing more attentions. Understanding the numerical error propagation is useful to examine the degree of approximation and feasibility of numerical algorithm for problems in many fields. For instance, Ferm and Lötstedt [1] have recently studied the numerical errors in the boundary conditions of the Euler equations of fluid flow by solving the error equations to analyse the propagation of the discretisation errors and in particular the errors caused by boundary conditions. It was reported that errors generated at a wall transported distinctly in subsonic and supersonic flows. Increasing the accuracy of boundary conditions and providing finer grid are possible strategy

*Correspondence to: Z. J. Zhu, Department of Thermal Science and Energy Engineering, University of Science and Technology of China, Anhui, Hefei, 230026, People's Republic of China.
†E-mail: zuojin@ustc.edu.cn

Received 2 October 2002
Accepted 19 November 2003

to reduce the errors. Preceding this error analysis, they have compared the convergent history in the solution of Euler equations for compressible flow between their iterative algorithm combining the blockwise adaptive grids with three-level multigrid acceleration and that obtained by other algorithms, through which it was indicated that their algorithm can treat with the compressible flow more efficiently [2].

Similarly, a posteriori error estimation for finite-volume solutions of shock wave equation was presented by Zhang *et al.* [3]. It was reported that the proposed error estimating technique can predict correctly the location and magnitude of the errors. An example concerned with boundary element method was given by Paulino *et al.* [4], while for error estimation involving with finite element method, Mathisen *et al.* [5] have made a relevant investigation. Zhu and Zienkiewicz [6, 7] have presented the superconvergence recovery technique and *posteriori* error estimates.

A literature review for the error quantification in computational fluid dynamics (CFD) can be found from the work of Roache [8], in which the verification, validation and related subject for CFD, including error taxonomy, error estimation and banding, convergence rate, surrogate estimators, non-linear dynamics, and error estimation for grid adaption vs quantification of uncertainty have been covered.

However, it is more evident to compare numerical results with its corresponding analytical counterpart for benchmark problems. For most non-linear problems, it is difficult to seek the analytical solutions. But by using transformations, it may be easy to write down the linear form of governing equations. For instance, Mychidinov *et al.* [9] have simplified linearly the governing equation single phase flow in porous media. In addition, for $1+1$ non-linear granular or traffic flow problems, it is likely to write the governing equations in linear form if the proper transformation may be sought. Based on these considerations, in order to see the numerical error patterns in the solution of a simpler problem, we focus on solving numerically $1+1$ linear wave equation with fourth-order accuracy based on Hermite interpolation. The time trains of errors were calculated from the numerical and analytical solutions. For the linear wave problem, it was found that a decrease of time step has not made an improvement of numerical solution.

2. THE GOVERNING EQUATIONS

Consider the $1+1$ linear wave problem with the governing equations

$$Lu = \frac{\partial^2 u}{\partial y^2} - \frac{\partial^2 u}{\partial t^2} = f(y,t) \tag{1}$$

where L is the linear operator. For simplicity, the forcing term $f(y,t)$ is assumed to be a constant, say $f(y,t) = -2$, but the initial conditions are assumed as

$$u(0,y) = y, \quad \frac{\partial u(0,y)}{\partial t} = 5y \tag{2}$$

together with boundary conditions given by

$$u(t,0) = 0, \quad u(t,1) = 1 \tag{3}$$

Referring to the Advanced Engineering Mathematical handbook [10], and using the variable separation algorithm, the analytical solution of above linear wave problem can be given by

$$u(t, y) = -y^2 + 2y + w(t, y) \tag{4}$$

where $w(y,t)$ is the general solution of linear wave equation without forcing effects. It can be written as

$$w(t, y) = \sum_{n=1}^{N\to\infty} [C_n \cos(n\pi t) + D_n \sin(n\pi t)] \sin(n\pi y) \tag{5}$$

where C_n and D_n are the coefficients of the Fourier series,

$$C_n = \frac{4}{(n\pi)^3} (\cos(n\pi) - 1), \quad D_n = -\frac{10}{(n\pi)^2} \cos(n\pi) \tag{6}$$

The analytical solution can be calculated by selecting a reasonable large summation superior N, so that the maximum root mean square (rms) value for any value of y compared with the solution for $N/2$ is very small. With this criteria of series truncation, the analytical solution can be obtained conveniently.

3. THE NUMERICAL SCHEME

For convenience, we use uniform grid system in which τ is the temporal interval, with h being the spatial interval. For a given point in the (t, y) plane ($t_j = j\tau$, $y_k = kh$), according to Hermite interpolation method, from the unknown variable $U(t, y)$, and operator LU, and the symmetry for the problem, the Hermite interpolation function Φ can be given by

$$\begin{aligned}\Phi = {} & a_0 U_{j,k} + a_1[U_{j+1,k} + U_{j-1,k}] + a_3[U_{j,k+1} + U_{j,k-1}] \\ & + a_4[U_{k+1,j+1} + U_{k+1,j-1} + U_{k-1,j+1} + U_{k-1,j-1}] \\ & + h^2\{b_0(LU)_{j,k} + b_1[(LU)_{j+1,k} + (LU)_{j-1,k}] + b_3[(LU)_{j,k+1} + (LU)_{j,k-1}] \\ & + b_4[(LU)_{j+1,k+1} + (LU)_{j+1,k-1} + (LU)_{j-1,k+1} + (LU)_{j-1,k-1}]\}\end{aligned} \tag{7}$$

Assuming the ratio of temporal to spatial interval as $\lambda = \tau/h$, taking $P_0(j\tau, kh)$ as the origin of the translated grid system, then interpolation Φ should be vanished when variable U is identical to $1, t^2, y^2, t^4, t^2, y^2$, and y^4 respectively. From these constrains for Φ, the following

algebraic equations can be used to identify the interpolation coefficients:

$$\begin{aligned} a_0 + 2a_1 + 2a_3 + 4a_4 &= 0 \\ 2\lambda^2 a_1 + 4\lambda^2 a_4 - 2b_0 - 4b_1 - 4b_3 - 8b_4 &= 0 \\ 2a_3 + 4a_4 + 2b_0 + 4b_1 + 4b_3 + 8b_4 &= 0 \\ 2\lambda^2 a_1 + 4\lambda^2 a_4 - 24b_1 - 48b_4 &= 0 \\ 4\lambda^2 a_4 + 4\lambda^2 b_1 - 4b_3 + (8\lambda^2 - 8)b_4 &= 0 \\ 2a_3 + 4a_4 + 24b_3 + 48b_4 &= 0 \end{aligned} \tag{8}$$

Let $\rho = 1/\lambda^2$, and δ denote an arbitrary parameter, the solution of above algebraic equations gives rise to

$$\begin{aligned} a_0 &= 20(\rho - 1), \quad b_0 = -8 - 4\delta \\ a_1 &= -(2 + 10\rho), \quad b_1 = -1 + 2\delta \\ a_3 &= 2\rho + 10, \quad b_3 = -1 + 2\delta \\ a_4 &= -(\rho - 1), \quad b_4 = -\delta \end{aligned} \tag{9}$$

Let $\beta = (h/\tau)^2 - 1$, from the coefficients of Hermite interpolation, the finite difference equations having fourth-order accuracy can be written as

$$\begin{aligned} &\frac{1}{h^2}\{[-\beta U_{j+1,k-1} - (12 + 10\beta)U_{j+1,k} - \beta U_{j+1,k+1}] \\ &\quad + [(12 + 2\beta)U_{j,k-1} + 20\beta U_{j,k} + (12 + 2\beta)U_{j,k+1}] \\ &\quad - [\beta U_{j-1,k-1} + (12 + 10\beta)U_{j-1,k} + \beta U_{j-1,k+1}]\} \\ &\quad + \{[\delta f_{j+1,k-1} + (1 - 2\delta)f_{j+1,k} + \delta f_{j+1,k+1}] \\ &\quad + [(1 - 2\delta)f_{j,k-1} + (8 + 4\delta)f_{j,k} + (1 - 2\delta)f_{j,k+1}] \\ &\quad + [\delta f_{j-1,k-1} + (1 - 2\delta)f_{j-1,k} + \delta f_{j-1,k+1}]\} = 0 \end{aligned} \tag{10}$$

or, alternatively

$$\frac{1}{h^2}\begin{pmatrix} -\beta & -12-10\beta & -\beta \\ 12+2\beta & 20\beta & 12+2\beta \\ -\beta & -12-10\beta & -\beta \end{pmatrix} U + \begin{pmatrix} \delta & 1-2\delta & \delta \\ 1-2\delta & 8+4\delta & 1-2\delta \\ \delta & 1-2\delta & \delta \end{pmatrix} LU = 0 \tag{11}$$

Since δ is an arbitrary scheme parameter, it is perceptively sensed that δ has no impact on the numerical solution. Actually, numerical calculation for the linear wave problem described in Section 2 has confirmed that the solution is completely rigid to the variation of scheme parameter δ. Hence, in numerical calculation, it is convenient to set δ as zero. For non-linear problems, if proper transformations can be used in the linearisation of governing equations, the scheme may be applied. Thus, despite its simplicity, this numerical study on the error patterns for Hermite interpolation scheme for $1+1$ linear wave equations, may have great significance in application.

4. RESULTS AND DISCUSSION

The following numerical results are obtained by the fourth-order finite difference scheme in terms of Hermite interpolation. The spatial step is $h=1/60$, and the corresponding time step is $\tau=h$, or $0.75h$. But when the sensitivity of temporal interval is concerned, another two values of $\tau=0.5h$, and 0.25 are used. Numerical experiments show that the solution process has diverged as long as the ratio λ is greater than unity.

The analytical solution is performed with the summation superior N $(=12\,800)$, which is evaluated from the criteria that the root means square of the deviation of the solution with superior N, for a given position y in the temporal period $t\in(0,10)$, from the solution with superior $N/2$ $(=6400)$ should be less than 10^{-5}. This solution can be seen from Figure 1(a). It has evident temporal periodical properties. The so-called numerical error is defined as the difference between the numerical and the analytical solutions.

For the $1+1$ linear wave problem, with the fourth-order scheme with Hermite interpolation, the numerical results indicate that despite the common perception (e.g. decreasing the temporal interval in case of given spatial intervals might be useful to improve the solution and reduce the numerical errors), the error pattern for the ratio $\lambda=1$ is regular (see, Figure 1(b)), and becomes irregular for the ratio $\lambda=0.75$ which can be seen from Figure 1(c).

For $\lambda=0.75$, Figure 1(c) shows that the error originated from the left-up corner can propagate along the characteristic lines. During the propagation process, the numerical error eventually appears a chaotic behaviour.

Figure 2 conveys the phase diagram for the problem (see Reference [11]), where parts (a) and (b) are given for the ratio $\lambda=1$, with parts (c) and (d) for the case $\lambda=0.75$. Figure 2(a) shows two error trajectories for the temporal error sequence for $y=0.2$ and 0.8, respectively. Except for the four-corner regions, both trajectories are almost mutually overlapped. Figure 2(b) shows the trajectory for the temporal error sequence for $y=0.5$. It is seen that for $\lambda=1$ the range of the error variation rate denoted by $\mathrm{d}E/\mathrm{d}t$ is almost positional independent. However, the orbits shown in the phase plane are approximately rectangles whose heights are almost identical, showing that the error range is spatially dependent, with its *maxima* less than 0.0085. Single error trajectory indicates that the error pattern is regular.

Different from what has seen found from Figures 3(a) and 3(b), Figures 3(c) and 3(d) show that for $\lambda=0.75$ apparent bunching of the trajectories for temporal error sequence for $y=0.2$, 0.8, and 0.5. The attractor is positioned at the origin of the phase plane, implying that the numerical solution has converged to the analytical one. However, chaotic effects make it difficult to clarify the definite trajectories.

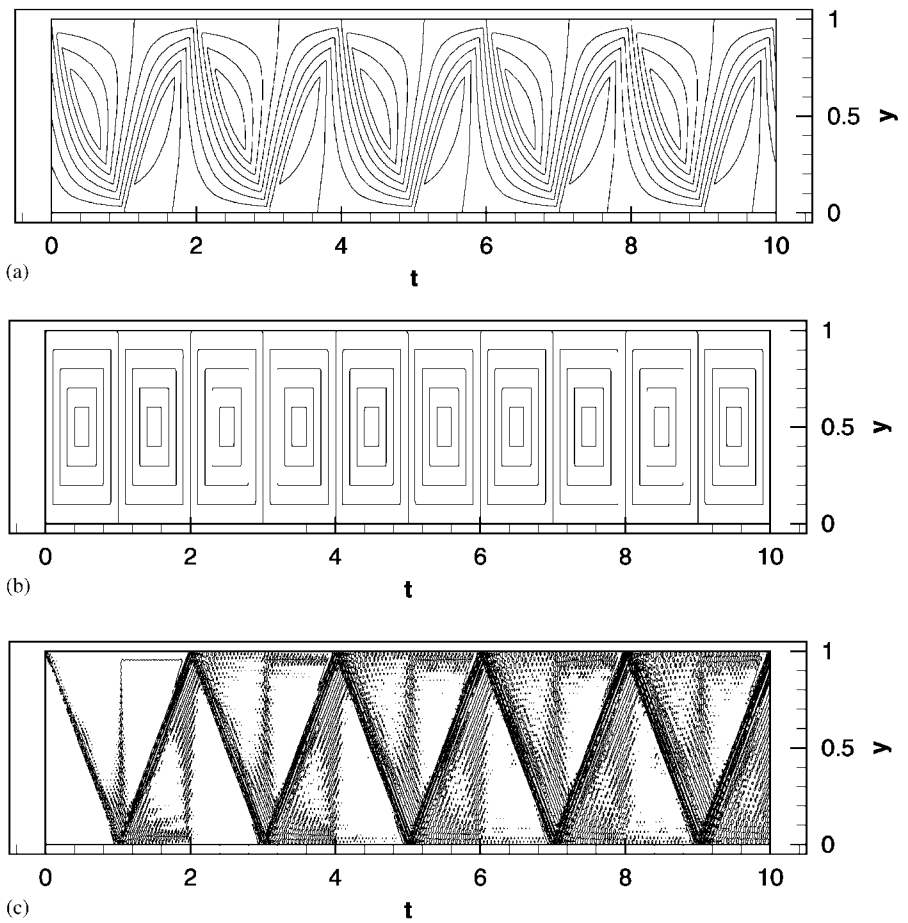

Figure 1. (a) Contours of the analytical solution, the curves are corresponding to $-0.25, 0, 0.25, \ldots, 1.75$ with an increment 0.25; (b) numerical error patterns for $\lambda = 1$, the error range is from -0.006635 to $+0.006635$; and (c) numerical error patterns for $\lambda = 0.75$, the error range is -0.02902–0.03017.

Corresponding to the illustration of the error trajectory in the phase plane, Figures 3(a) and 3(b) show the evolution of numerical error for the ratio $\lambda = 1, 0.75$, and $y = 0.2$. There exist terraced periodic waves for the case of $\lambda = 1$. The wavelength is 2. However, heart pumping type waves can be observed for the case $\lambda = 0.75$, as shown in Figure 3(b). Apart from the evident larger pulse with a time interval of 0.4, there are small oscillations with varying magnitudes, reflecting the presence of numerical chaos.

Figure 4 illustrates the distribution of Hurst index along the y direction for four cases. According to Reference [12], Hurst index is defined as ratio between the difference of *maxima* and *minima* of cumulative temporal sequence to the root mean square of the temporal sequence. If the sequence is not self-correlated, the value of Hurst index should equal 0.5; when it is positively self-correlated, the Hurst index is larger than 0.5; otherwise the Hurst index should less than 0.5. From Figure 4, the error analysis indicates that the choice of λ has

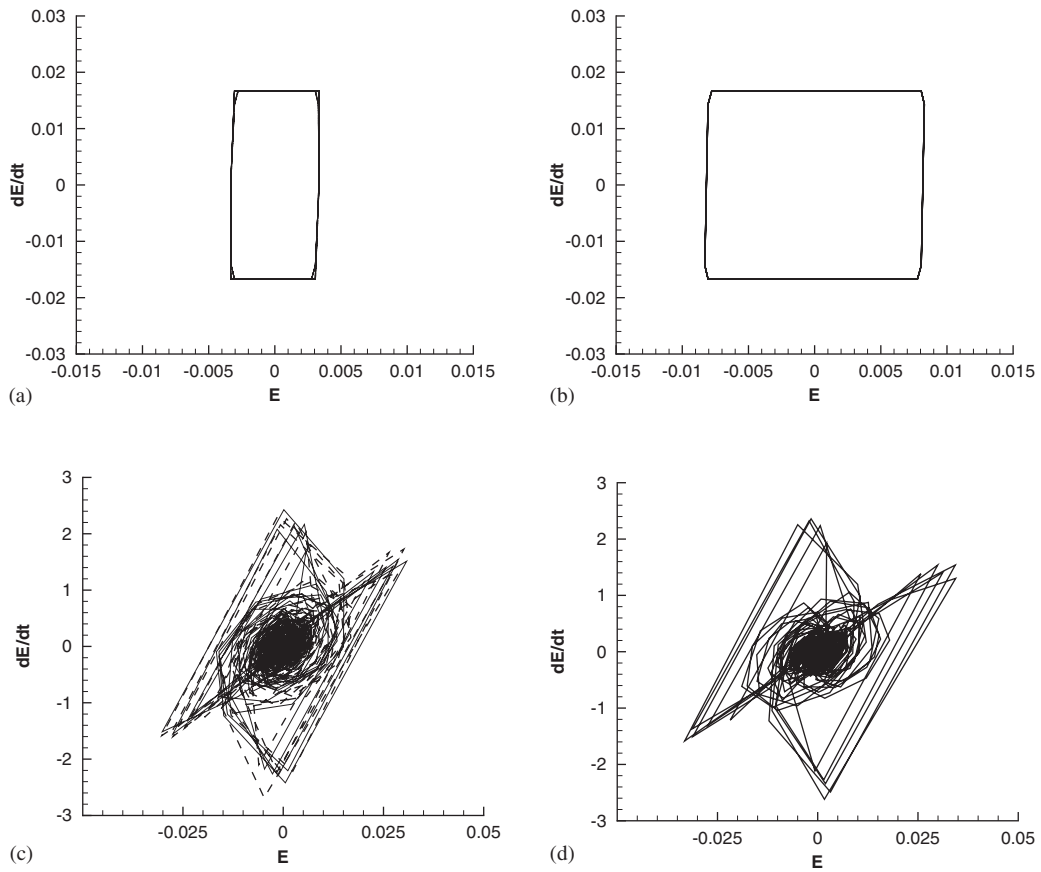

Figure 2. Phase diagram for numerical errors, where: (a) for $\lambda = 1$, and $y = 0.2$ and 0.8, in which the trajectory for $\lambda = 0.8$ is denoted by thin solid line; (b) for $\lambda = 1$, and $y = 0.5$; (c) for $\lambda = 0.75$, and $y = 0.2$ and 0.8, in which the trajectory for $\lambda = 0.8$ is denoted by thin solid line; and (d) for $\lambda = 0.75$, and $y = 0.5$.

greater influence on the Hurst index distribution. It appears that the time sequence of numerical error is always positively self-correlated when $\lambda = 1$, the Hurst index is about 0.63 whose maximum deviation is close to 0.01. However, when $\lambda = 0.25$, 0.5, and 0.75, the situation of self-correlation becomes spatially dependant. In the central region of y, the Hurst index is greater than 0.5, implying the presence of positive self-correlation, but in both sides regions, it shows a negative self-correlation. Note that in this case the distribution of Hurst index appears an oscillating property, the value of Hurst index at an arbitrary point is less than 0.6.

5. CONCLUSIONS

This paper presents the numerical error patterns occurred in the solution of $1 + 1$ linear wave equation obtained by using a fourth-order scheme with Hermite interpolation. It was found that

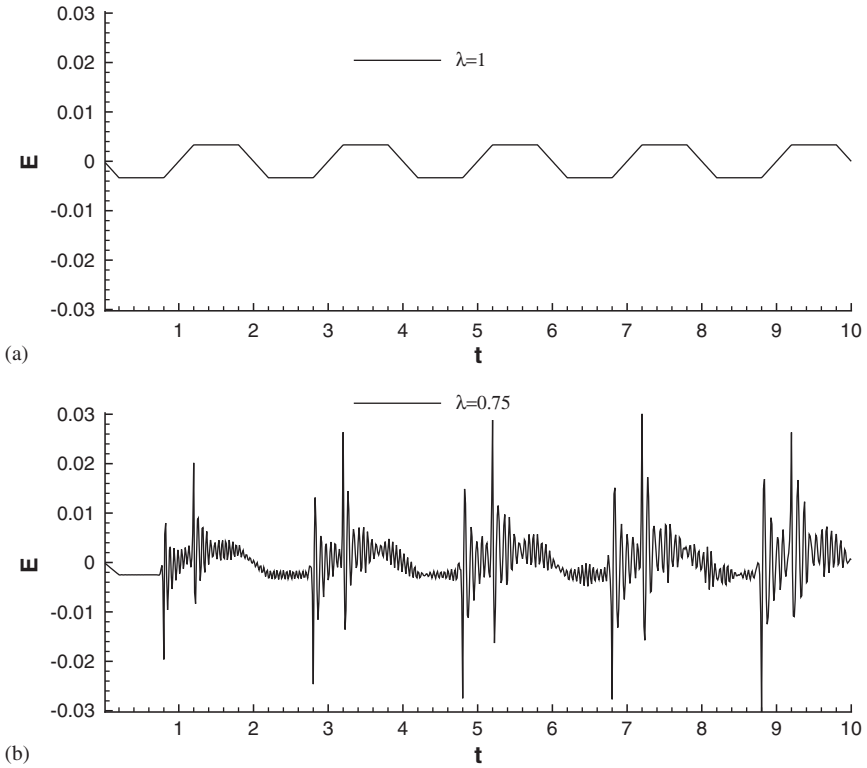

Figure 3. Evolution of numerical error E for the case $y = 0.2$, where: (a) when λ equals unity; and (b) when λ equals 0.75.

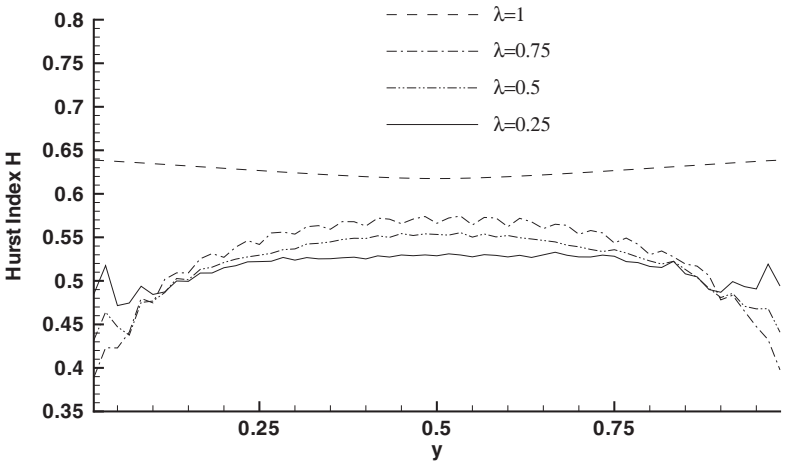

Figure 4. Distribution of Hurst index along the y direction.

this numerical scheme cannot perform convergent solutions for the problem when the ratio of temporal to spatial intervals is greater than unity, it is only valid when the ratio is less than unity. There is no chaotic properties in the numerical error propagation process when the ratio is unity. Despite the common perception that decreasing temporal interval might improve the numerical solution, the numerical results show that for the problem on hand the better choice of the ratio may be unity; otherwise chaotic patterns in the propagation of numerical error can appear. That means, when the temporal interval is less than spatial interval, the error pattern can be fully irregular, and bifurcation and chaos of numerical error can be seen from the phase diagrams.

ACKNOWLEDGEMENTS

The author thanks the anonymous referees for their very helpful comments.

REFERENCES

1. Ferm L, Lötstedt P. On numerical errors in the boundary conditions of the Euler equations. *Applied Mathematics and Computation* 2002; **128**:129–140.
2. Ferm L, Lötstedt P. Blockwise adaptive grids with multigrid acceleration for compressible flow. *AIAA Journal* 1999; **37**(1):121–122.
3. Zhang XD, Trépanier JY, Camarero R. A posteriori error estimation for finite-volume solutions of hyperbolic conservation laws. *Computer Methods in Applied Mechanics and Engineering* 2000; **185**:1–19.
4. Paulino GH, Menon G, Mukherjee S. Error estimation using hypersingular integrals in boundary element methods for linear elasticity. *Engineering Analysis with Boundary Elements* 2001; **25**:523–534.
5. Mathisen KM, Hopperstad OS, Okstad KM, Berstad T. Error estimation and adaptivity in explicit nonlinear finite element simulation of quasi-static problems. *Computers and Structures* 1999; **72**(4–5):627–644.
6. Zhu ZJ, Zienkiewicz OC. Superconvergence recovery technique and posteriori error estimates. *International Journal for Numerical Methods in Engineering* 1990; **30**:1321–1339.
7. Zienkiewicz OC, Zhu ZJ. The superconvergent path recovery and posteriori error estimates, I: The recovery technique. *International Journal for Numerical Methods in Engineering* 1992; **33**:1331–1364.
8. Roache P. Quantification of uncertainty in computational fluid dynamics. *Annual Review of Fluid Mechanics* 1997; **29**:123–160.
9. Mychidinov N, Mykimov N, Cadeikov MK. *Numerical Simulation of Non-linear Filtration*. Fan Publisher: Tashkent, 1989; 52–59 (in Russian).
10. Kreyszig E. *Advanced Engineering Mathematics* (8th edn). Wiley: New York, 1999.
11. Huang NE, Zheng S, Steven RL. A new view of nonlinear water waves: the Hilbert Spectrum. *Annual Review of Fluid Mechanics* 1999; **31**: 417–457.
12. Chen Y, Chen L. *Fractal Geometry*, Chapter 7. Chinese Earthquake Publisher: Beijing, 1998; 145–150 (in Chinese).

